LAMS-2482

LOS ALAMOS SCIENTIFIC LABORATORY

OF THE UNIVERSITY OF CALIFORNIA o LOS ALAMOS NEW MEXICO

TURRET PRELIMINARY NUCLEAR CALCULATIONS

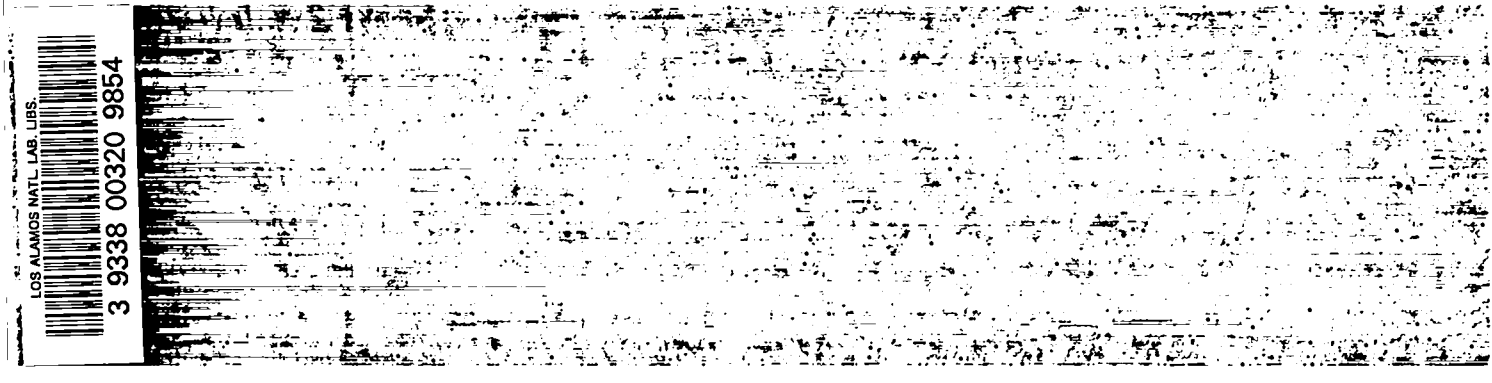

LEGAL NOTICE

Printed in USA. Price $ 1.00. Available from the

Office of Technical Services
U. S. Department of Commerce
Washington 25, D. C.

LAMS-2482
REACTORS - GENERAL
(TID-4500, 15th Ed.)

LOS ALAMOS SCIENTIFIC LABORATORY
OF THE UNIVERSITY OF CALIFORNIA LOS ALAMOS NEW MEXICO

REPORT WRITTEN: December 1, 1960

REPORT DISTRIBUTED: March 2, 1961

TURRET PRELIMINARY NUCLEAR CALCULATIONS

Work done by:

M. E. Battat
B. M. Carmichael
R. J. La Bauve
M. Wilson
W. Schmedt, Sandia Corporation

Written by:

B. M. Carmichael
R. E. Peterson

Contract W-7405-ENG. 36 with the U. S. Atomic Energy Commission

ABSTRACT

A preliminary study of the nuclear parameters of the Turret reactor is described. It is estimated that at the design operating temperature of 1350°C and power of 3 MW (Thermal) the critical mass will be 7.1 kg of highly enriched uranium. An estimate of 21% Δk is obtained for the amount of shutdown control needed, and it is calculated that the proposed three-ring control rod system will provide 28% Δk shutdown control. A slow negative temperature reactivity coefficient of 1.4×10^{-4} $(\Delta k/k)/°C$ is found, and a negative prompt reactivity coefficient of the order of 10^{-5} $(\Delta k/k)/°C$ is envisioned.

ACKNOWLEDGEMENTS

In performing Turret calculations maximum use has been made of the generalized reactor codes, DSN[1] and FIRE,[2] which have been developed by staff members of T-1, LASL. The authors wish to acknowledge in particular the considerable assistance rendered by B. Carlson, C. B. Mills, F. Brinkley, L. Stone, and M. Riedel in the application of these codes to the Turret problem.

CONTENTS

I. Introduction

Calculations of the nuclear parameters of importance in the design of Turret have to date been mostly of a preliminary nature, with the aim of uncovering any gross incompatibilities between the nuclear and mechanical requirements of the proposed systems. A program of refining the critical calculations is now developing as material specifications, mechanical details, and heat transfer data become available. The scope of the first calculations will be outlined in this introductory section, and the planned refinements noted; a more detailed presentation of the results of the calculations is given in the following sections.

When the Turret project started, the need for critical experiments was considered. The final decision not to do any critical mockups was based on two factors. First, there was available data from previous LASL critical measurements on a graphite moderated, highly enriched U-fueled system (Honeycomb) of a size and composition comparable to the Turret conceptual design. Second, the very earliest estimates indicated that the fuel loading required for Turret criticality would be roughly one-half the upper limit attainable by solution impregnation of the graphite fuel-bearing elements which were the basis of the Turret concept. Thus it appeared that if the available experimental data could be reproduced by calculation, extrapolation of these computational methods to Turret design should be satisfactory in view of the safety factor available by a simple change in Turret fuel concentration during startup tests. Experimentally verified information on control rod worths would have been useful during Turret design, but the decision has been made to base control element specification on a conservative evaluation of calculations.

The first step in the calculational program was to calculate k_{eff} for the available critical assembly data. k_{eff} for the critical system was computed to be about 1.05, and this value was taken as the "normalized" k_{eff} which would correspond to the critical configuration in Turret calculations.

A first model for the actual Turret configuration was then selected on the basis of heat removal and mechanical criteria. Using preliminary graphite specification data, densities and parasitic absorption cross sections

were chosen. Fuel concentration in the reactor was assigned a radial variation corresponding to about 50% burnup as fuel passed through the system. To simplify computation, the 18 group cross sections used in the normalization of k_{eff} were collapsed to 5 groups. k_{eff} on this Turret-like system at 1350°C was then computed as a function of fuel concentration ($0.73 < k_{eff} < 1.08$). The critical loading ($k_{eff} \cong 1.05$) was found to be ~0.08 g/cc, or 4.6 gm/fuel element (7.1 kg total). Flux plots from this first calculation were used to estimate power distribution for the isothermal core. A preliminary value for the reactivity worth of a fuel element was also obtained; worth per element was so small that no problems were anticipated in reloading the reactor at power.

Estimates were next made of the system's isothermal temperature coefficients of reactivity by comparing k_{eff} at 1350°C and 20°C (isothermal temperature distributions). Variation of cross sections with temperature, as well as the temperature-induced changes of material density, were considered. It was found that a Δk of 0.21 must be provided to shut the reactor down to room temperature when it was loaded for criticality at 1350°C. At this stage of the calculations only the average isothermal temperature coefficient over the entire range of temperatures (startup to full power) was investigated, and no detailed prediction of the reactivity coefficient in the vicinity of operating temperature was made. It was also found, as expected, that prompt reactivity effects associated with fuel temperature are small, the main reactivity effect being associated with changes in moderator temperature. The transient behavior of the system will be, therefore, determined by the heat-flow coupling between the fuel elements and the moderator. No temperature-dependent fission product poisoning was considered in these first estimates of temperature coefficients.

On the basis of these preliminary estimates of control requirements, the reactivity worth of some suggested control rod configurations was computed. The first scheme studied involved rods in the central plug of the core, and a "curtain" of neutron absorber between the rotatable core and the stationary reflector. It appeared that this layout provided a satisfactory amount of control, but upon re-examination, the mechanical features and material restrictions appeared unacceptable. A method for introducing rods into the moveable core, as well as into the stationary central plug and outer reflector, was devised; and further calculations indicated that the selected control element material, ZrB_2, would give a reasonable amount of control.

Better information on materials density, mechanical design of the core and reflector region, etc., became available as these calculations continued. The basic critical mass estimates were repeated with new parameters. Such factors as increased moderator and reflector densities, extension of the calculational model to include the porous carbon thermal insulation surrounding

the reflector, etc., indicated that the critical mass might be decreased by ~25% from that first estimated; similarly, the substitution of a radially uniform fuel concentration for the "simulated-burnup" loading would produce a flatter power distribution and a further decrease in critical mass. It is expected, however, that the effects of fission product poisons, gaps in the reflector, gas plenums, etc., will about offset these increases in k_{eff}, so that the final value of the critical mass will not be greatly different from the 7.1 kg first obtained.

Refinements to the idealized, isothermal problems are now underway. The temperature distribution of the reactor at rated power has been estimated, and the control requirements for this case will be computed, taking into account fission product poisoning effects which are temperature dependent because of cross section dependence on temperature. The power coefficient of the system will also be estimated, and better estimates of the isothermal temperature coefficient will be made considering in greater detail the structure of the core, reflector, and insulating carbon.

Transient behavior of the system has been given only casual attention so far. One of the basic problems is the obtaining of data on fission product retention as a function of fuel element temperature. The interrelation of negative temperature coefficients of nuclear origin and the reactivity effects associated with the loss or migration of fission product poison during a temperature excursion can not be evaluated until reasonable assumptions as to fission product diffusion rates can be made.

II. Criticality Calculations

1. Normalization. The Honeycomb assembly used as the reference critical experiment consisted of a core in the form of a four foot cube; it was reflected on all sides by one foot of graphite of density 1.55 g/cc.[3] The critical core consisted of 7.98 kg of Oy (93.5% U^{235}, 6.5% U^{238}) in the form of foils (0.001 in. by 2.8 in. by 7.5 in.) which were distributed uniformly through graphite of density 1.50 g/cc. The structural Al in the Honeycomb assembly had an effective density of 0.165 g/cc in the core and reflector. The fuel region C/Oy atomic ratio of 6650 corresponded roughly to the average C/Oy ratio in Turret.

In the calculation of k_{eff} for the above experiment, C. B. Mills' 18 group cross-sections were used.[4] A technique for applying results from the one-dimensional FIRE code to the experimental cubic geometry was similar to that later used in Turret calculations. To start the calculations, artificial g-th group absorption cross sections

$$\Sigma_g^a = 2\, D_g\, B^2 \qquad (1)$$

were used in a plane calculation to mock up side leakage. D_g in Eq. 1 is the group diffusion coefficient for the g-th group and B^2 is an approximate buckling obtained from

$$B^2 = \pi^2 / \left(H_c + H_r\right)^2 \qquad (2)$$

where H_c and H_r are the core thickness and total reflector thicknesses, respectively.

From the flux distributions, φ_g, obtained from the first plane calculation, new leakage cross-sections were computed using

$$\Sigma_g^a = - \frac{2\, D_g \left(\frac{d\,\varphi_g}{dz}\right)_{H_c/2}}{\int_0^{H_c/2} \varphi_g \, dz} \qquad (3)$$

in which the slope of the flux φ_g is evaluated at the core boundary, $H_c/2$, for the symmetric plane case. Equation 3 represents the core leakage per (cm^3) of core transverse to the one dimension of calculation, and it may be shown that, for solutions $F(B_g z)$ to the diffusion equation, Eq. 3, reduces to $\Sigma_g^a = 2D_g B_g^2$. The Σ_g^a from Eq. 3 were then inserted into a second plane calculation, replacing those obtained from Eq. 1. After a third plane calculation, using the fluxes obtained from the second calculation to recompute the Eq. 3 cross-sections, k_{eff} converged to a value of 1.111.* After making the experimentally determined correction for the Oy foil self-shielding ($\Delta k_{eff} = -0.067$), a net k_{eff} of 1.044 was obtained for the Honeycomb critical experiment. Although the disagreement may be due to other inhomogeneities in the experiment which were neglected in the calculation, critical calculations for Turret have been normalized to a $k_{eff} \sim 1.05$.

2. Neutron Group Reductions. In order to reduce the labor involved in the Turret calculations, the 18 group cross-sections used in the normalization were collapsed to five groups using a procedure described in A.N.L.

---

*This method of computing the transverse group leakages has been used by other authors. See, for example, reference 5.

5800, p. 411.[6] From a preliminary 18-group Turret calculation, group weighting factors

$$d_g = U_g \varphi_g / \sum_{g \text{ in } G} U_g \varphi_g \tag{4}$$

were formulated. In Eq. 4, g and G refer to the 18 and 5 group sets, respectively; and U_g and φ_g are lethargy widths and fluxes per unit lethargy, respectively. The weighting factors were used in the following formulae:

Fission and absorption cross-sections:

$$\sigma_G = \sum_{g \text{ in } G} d_g \sigma_g \tag{5}$$

Transport cross-sections:

$$\sigma_G = 1/ \sum_{g \text{ in } G} \left(d_g / \sigma_g \right) \tag{6}$$

Transfer cross-sections:

$$\sigma_{G \to G'} = \sum_{g \text{ in } G} d_g \sum_{g' \text{ in } G'} \sigma_{g \to g'} \tag{7}$$

Fission Spectrum, lethargy widths and fluxes:

$$X_G = \sum_{g \text{ in } G} X_g \tag{8}$$

Maxwellian-averaged values for the thermal. fission and absorption cross-sections at 1350°C were calculated using

$$\sigma(T) = \left(\pi \ T_0 / 4T \right)^{1/2} g(T) \ \sigma_0 \tag{9}$$

In Eq. 9 σ_0 is the cross-section at 2200 meters per sec, T_0 and T represent

20°C and 1350°C expressed in °K, respectively, and g(T) is the non-1/v correction factor given in ANL-5800, p. 79.[6] The five-group parameters as computed using Eqs. 4 through 9 are listed in Table I.

3. First Turret Geometry. The calculational model first used for Turret is illustrated in Fig. 1. The core was a graphite cylinder of height 37.5 in. and outer radius 36.32 in. containing 312 radial fuel channels. The region from radius zero to 6.94 in. contained 79% graphite by volume and 21% void. The fuel channels were located in 13 equally spaced horizontal planes with each plane containing 24 radial channels. Each fuel channel contained five fuel elements which were graphite cylinders of length 5-7/8 in., 1 in. o.d., and 1/2 in. i.d. The channel i.d.'s were 1.1 in.

For calculational purposes the core was divided into five radial regions of equal width corresponding to the five fuel elements per channel. These are designated as Regions 2 through 6, Region 2 being the innermost core region. The inner graphite zone (r = 0 to r = 6.94 in.) described above was designated as Region 1. The concentration of Oy in the fuel elements of each radial region were selected according to the following prescription in order to approximate 50% burnup in the fuel elements as the fuel moves through the reactor:

Region	2	3	4	5	6
Concentration	4/6 c	5/6 c	c	7/6 c	8/6 c

The concentration c (in grams of Oy per cc of graphite), and hence the critical mass, was the parameter which was varied in the calculations for criticality.

In the calculations all the radial regions were homogenized. This neglected the self-shielding of the fuel which was estimated to affect $|k_{eff}| < 0.02$. A perturbation that was taken into account was the effect of contaminants in the graphite. It was assumed that type H4LM graphite would be used in fabricating Turret components. From the contaminant specifications for this graphite[7] it was estimated that the thermal absorption contributed by the contaminants was about equal to the thermal absorption due to the carbon. The contaminants were mocked-up in the calculations by inserting an amount of boron giving the same thermal absorption.

The seventh radial region in the problem, of radial thickness 15.7 in., was the radial graphite reflector. Top and bottom reflectors were 16.3 in. thick graphite. The graphite density was assumed to be 1.6 g/cc throughout.

4. Procedure for First Criticality Calculations. The procedure used in calculating Turret problems was similar to the method used in the normalization calculation. An infinite cylinder problem, containing the seven

TABLE I

FIVE GROUP PARAMETERS

Group	Energy Range	u_g*	U_g**	Fission Spectrum
1	10 Mev - 900 kev	2.408	2.408	0.716
2	900 kev - 17 kev	6.377	3.969	0.284
3	17 kev - 61.44 ev	12	5.623	0
4	61.44 ev - 0.14 ev	18.09	6.09	0
5	Thermal	---	1	0

FIVE GROUP CROSS-SECTIONS

Element	Group	σ_a	σ_{TR}	σ_f	$\sigma^{inel}_{g,g+1}$	$\sigma^{inel}_{g,g+I(I>1)}$
Boron	1	5.170 - 02	1.830 + 00	0	2.469 - 01	0
	2	3.947 - 01	2.501 + 00	0	1.612 - 01	0
	3	5.475 + 00	7.244 + 00	0	1.034 - 01	0
	4	4.581 + 01	3.888 + 01	0	1.555 - 01	0
	5	2.779 + 02	2.814 + 02	0	0	0
Carbon	1	0	1.549 + 00	0	2.402 - 01	0
	2	0	2.880 + 00	0	1.747 - 01	0
	3	0	4.367 + 00	0	1.275 - 01	0
	4	2.083 - 04	4.340 + 00	0	1.892 - 01	0
	5	1.178 - 03	4.828 + 00	0	0	0
U^{235}	1	1.303 + 00	4.505 + 00	1.312 + 00	1.137 + 00	0
	2	2.393 + 00	7.327 + 00	1.986 + 00	2.178 - 02	0
	3	1.433 + 01	2.148 + 01	1.008 + 01	1.724 - 02	0
	4	7.372 + 01	7.063 + 01	4.004 + 01	1.296 - 02	0
	5	2.311 + 02	2.411 + 02	1.908 + 02	0	0
U^{238}	1	4.295 - 01	4.367 + 00	3.968 - 01	1.582 + 00	0
	2	2.839 - 01	7.389 + 00	0	4.356 - 02	0
	3	4.711 + 00	1.643 + 01	0	1.379 - 02	0
	4	5.715 + 01	6.301 - 01	0	1.815 - 02	0
	5	1.013 + 00	1.001 + 01	0	0	0
DB^2***	1	2.278 - 01	0	0	0	0
	2	1.225 - 01	0	0	0	0
	3	8.081 - 02	0	0	0	0
	4	8.132 - 02	0	0	0	0
	5	7.310 - 02	0	0	0	0

*u_g = lethargy of lower energy limit of group

**U_g = group lethargy width

***Used in conjunction with Eq. 1

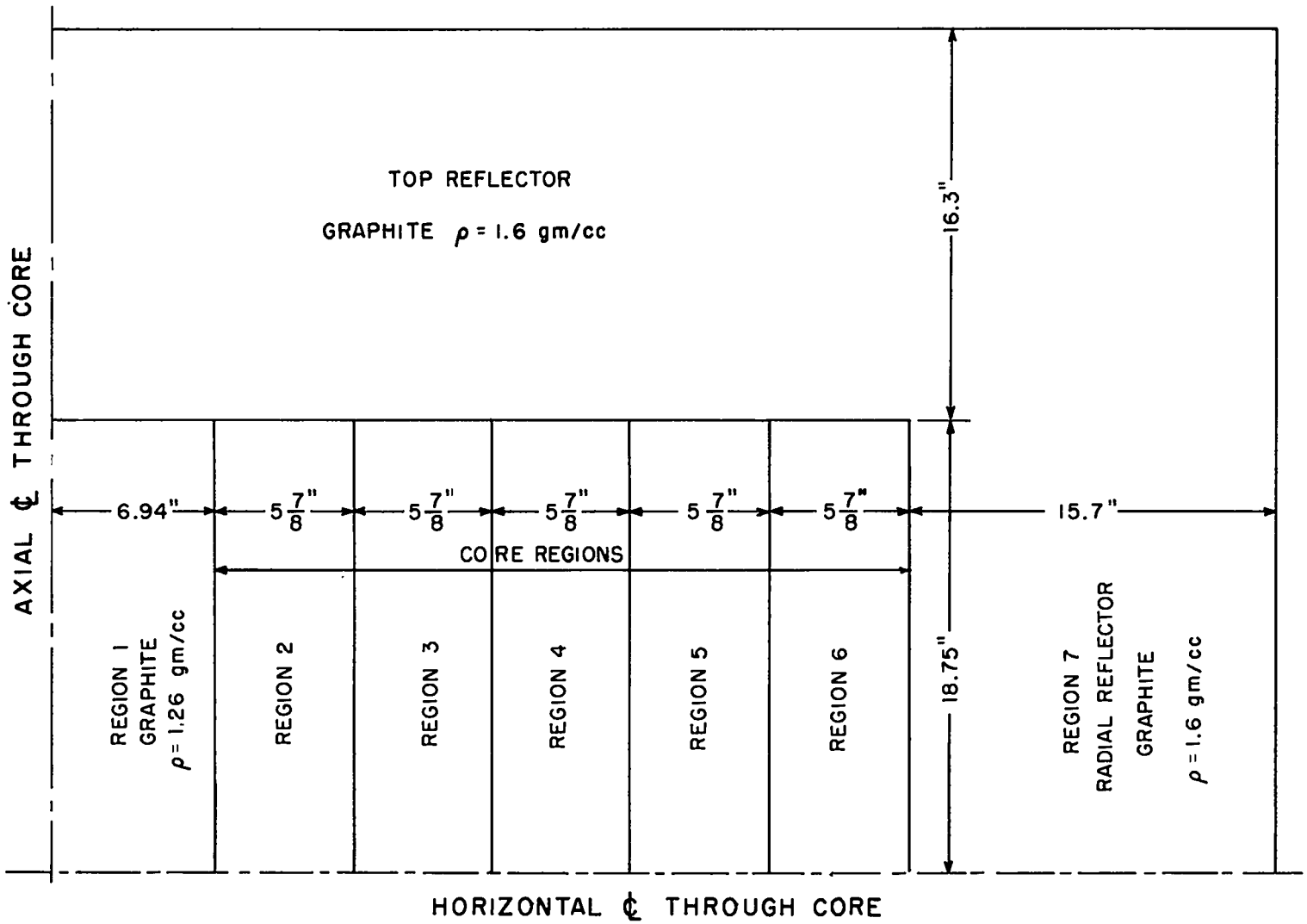

Fig. 1 Turret calculational model.

homogenized radial regions previously described, was first computed using the Eq. 1 approximation for the vertical leakage. From the radial fluxes, φ_{rg}, generated by the first cylinder problem, radial leakage cross-sections were computed for each of the five core regions from

$$\Sigma_g^a = \frac{D_g\left(r_1 \left.\frac{d\varphi_{rg}}{dr}\right|_{r_1} - r_2 \left.\frac{d\varphi_{rg}}{dr}\right|_{r_2}\right)}{\int_{r_1}^{r_2} \varphi_{rg}\, r dr} \qquad (10)$$

In Eq. 10, r_1 and r_2 are the inner and outer region radii, respectively.

An infinite plane problem was next computed, using the Turret vertical dimensions, for each of the five core regions. The radial leakage cross-sections (previously generated in the cylinder problem) for each given region were added as absorption cross-sections to the core material cross-sections for the region. Vertical leakage cross-sections were then obtained from the plane problems using Eq. 3. Finally, the infinite cylinder problem was re-computed using the new vertical leakage cross-sections in place of those computed by Eq. 1.

5. Results of First Criticality Calculations. Four calculations were performed in order to obtain a curve of k_{eff} versus total Oy mass. The results are given in Table II.

TABLE II

CALCULATED k_{eff} VERSUS TOTAL OY MASS

Problem Number	Oy Mass (kg)	k_{eff}	Temperature (°C)
42F	3.06	0.732	1350
41F	5.11	0.967	1350
43F	7.10	1.055	1350
40F	7.65	1.072	1350

The above data are plotted in Fig. 2. In the vicinity of case 43F the relation

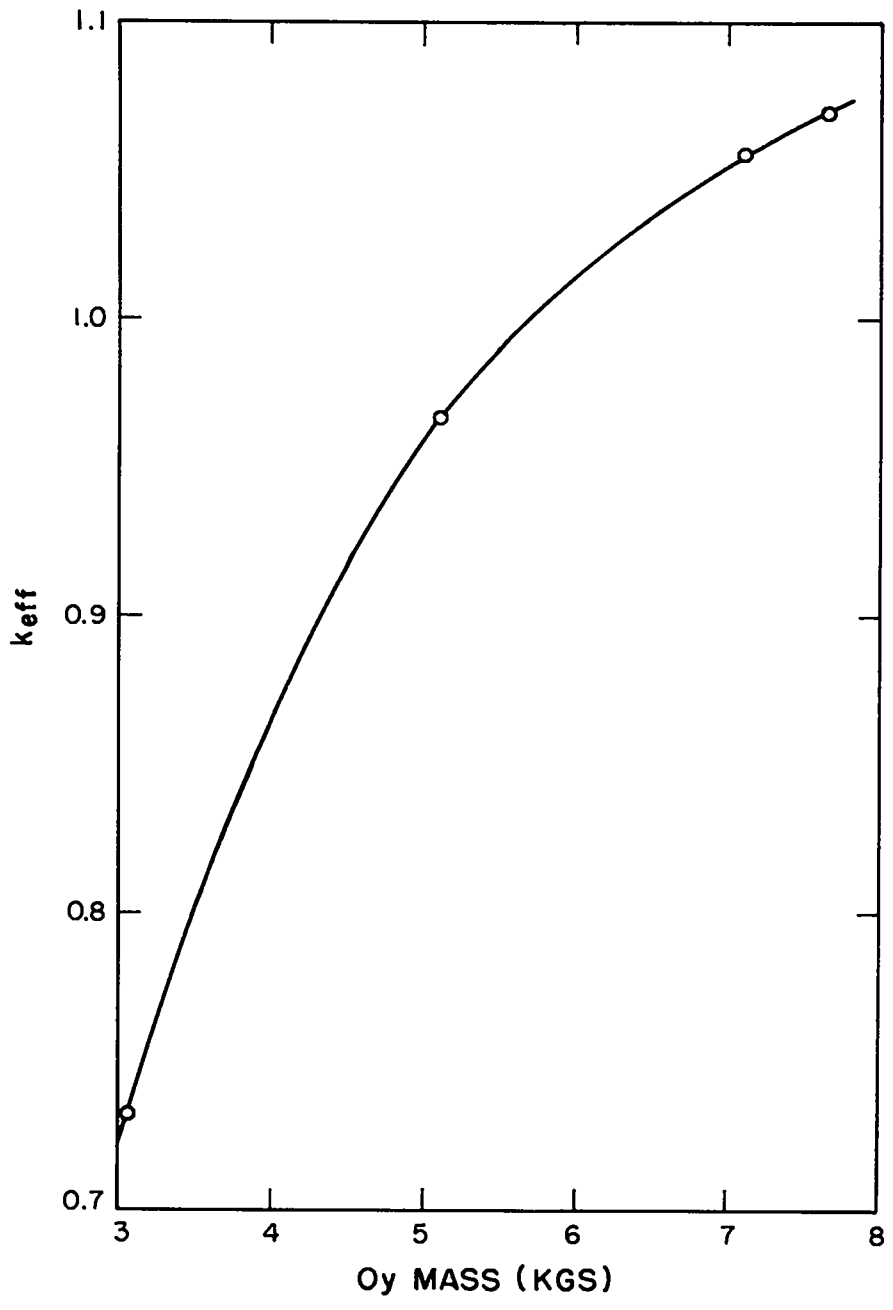

Fig. 2 k_{eff} vs Oy mass at 1350°C.

$$\Delta k_{eff}/k_{eff} = 0.21\ \Delta M/M \qquad (11)$$

is obtained. Case 43F has been adopted as the standard critical-configuration for flux and power plots, and for future computations based on the same geometry. The fuel concentration, c, for this case is 0.08 g/cc. The maximum concentration which may be conveniently attained during fuel element impregnation is about 0.15 g/cc.

Five-group fluxes from case 43F are plotted in Figs. 3 through 8. Radial fluxes are given in Fig. 3 and the vertical fluxes for Regions 2 through 6 are plotted in Figs. 4 through 8, respectively. The vertical fluxes were normalized to the radial fluxes by setting the average vertical flux for a given group and region equal to the average radial flux for the group and region. All fluxes correspond to a power of 3 MW.

It is seen that the thermal flux strongly predominates in the Turret system. The central peak in the radial thermal flux indicates that the central region will be the most valuable position for inserting control rods.

Table III contains a listing of the power produced per fuel element. In the table, channel 0 designates a channel in the horizontal plane passing through the core center, and the off-center channels are designated by 1 through 6 in the order of their proximity to the center. The radial variation

TABLE III

POWER PRODUCED PER FUEL ELEMENT (kw)

Reactor Power - 3 MW

Channel	Reactor Region 2	3	4	5	6	Channel Total
0	1.867	2.166	2.334	2.287	2.077	10.731
1	1.852	2.147	2.312	2.266	2.058	10.635
2	1.808	2.092	2.251	2.205	2.001	10.357
3	1.739	2.006	2.154	2.107	1.909	9.915
4	1.660	1.908	2.042	1.994	1.802	9.406
5	1.557	1.778	1.893	1.840	1.651	8.719
6	1.471	1.668	1.762	1.699	1.507	8.107

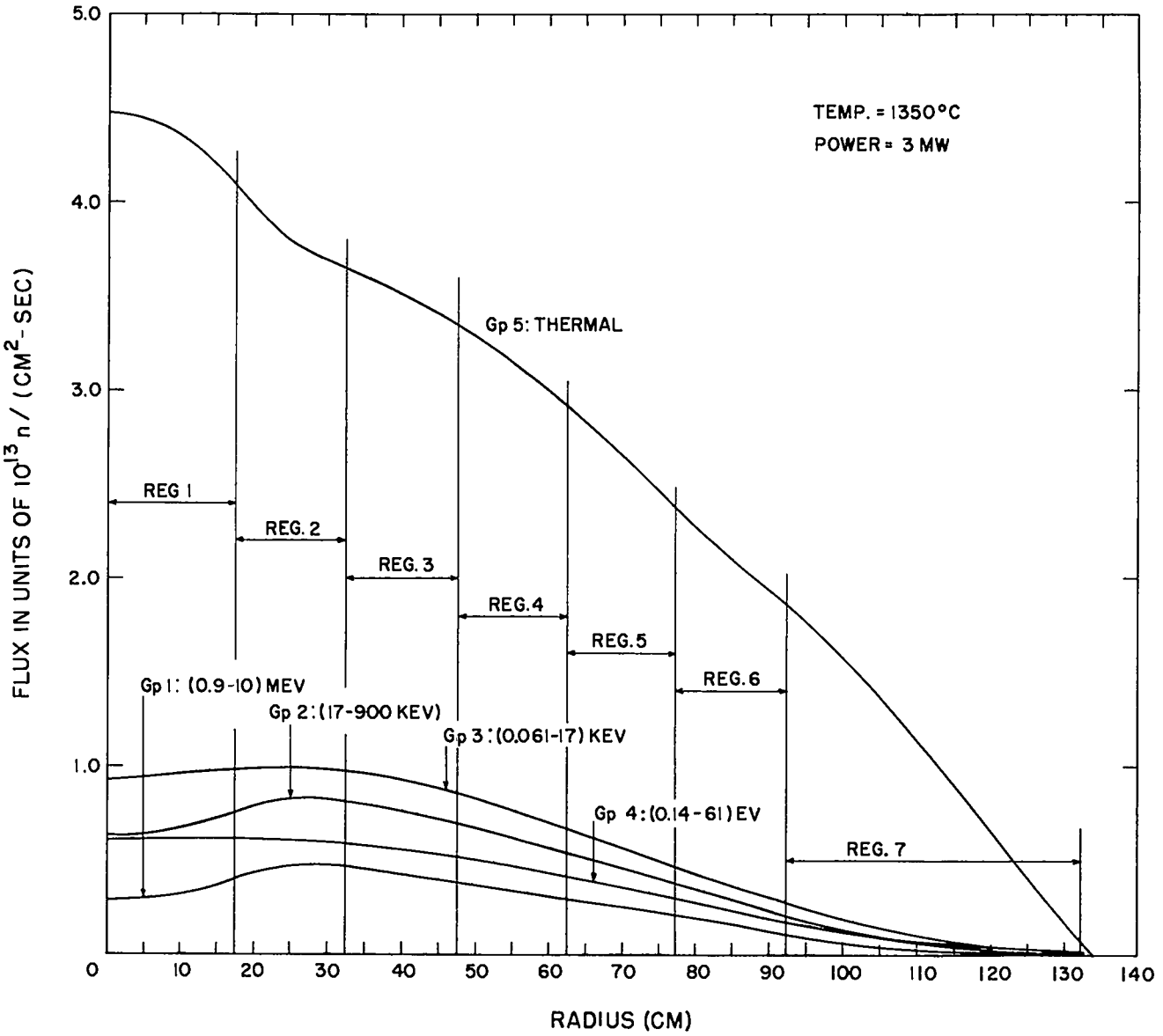

Fig. 3 Turret radial fluxes.

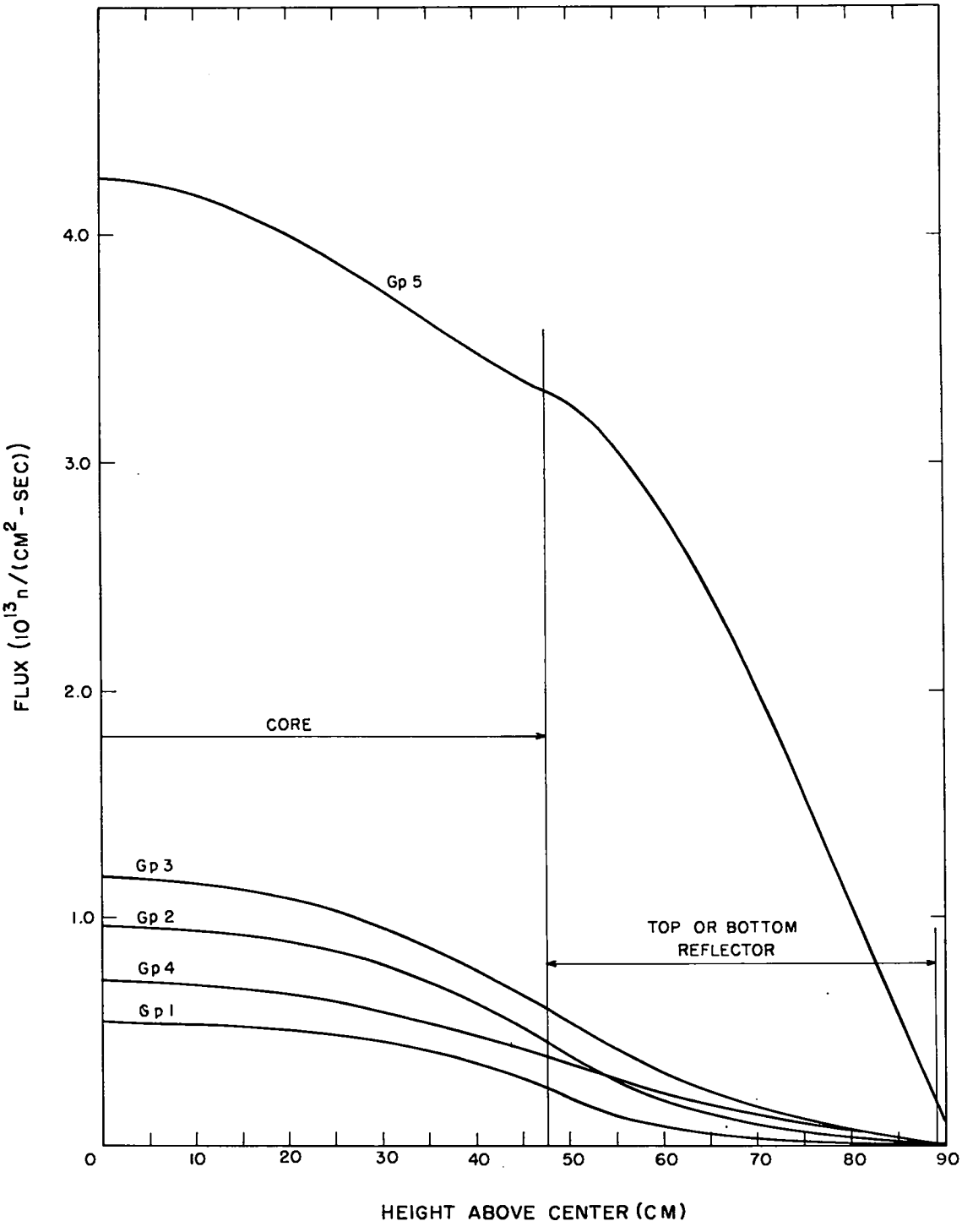

Fig. 4 Vertical fluxes, Region 2.

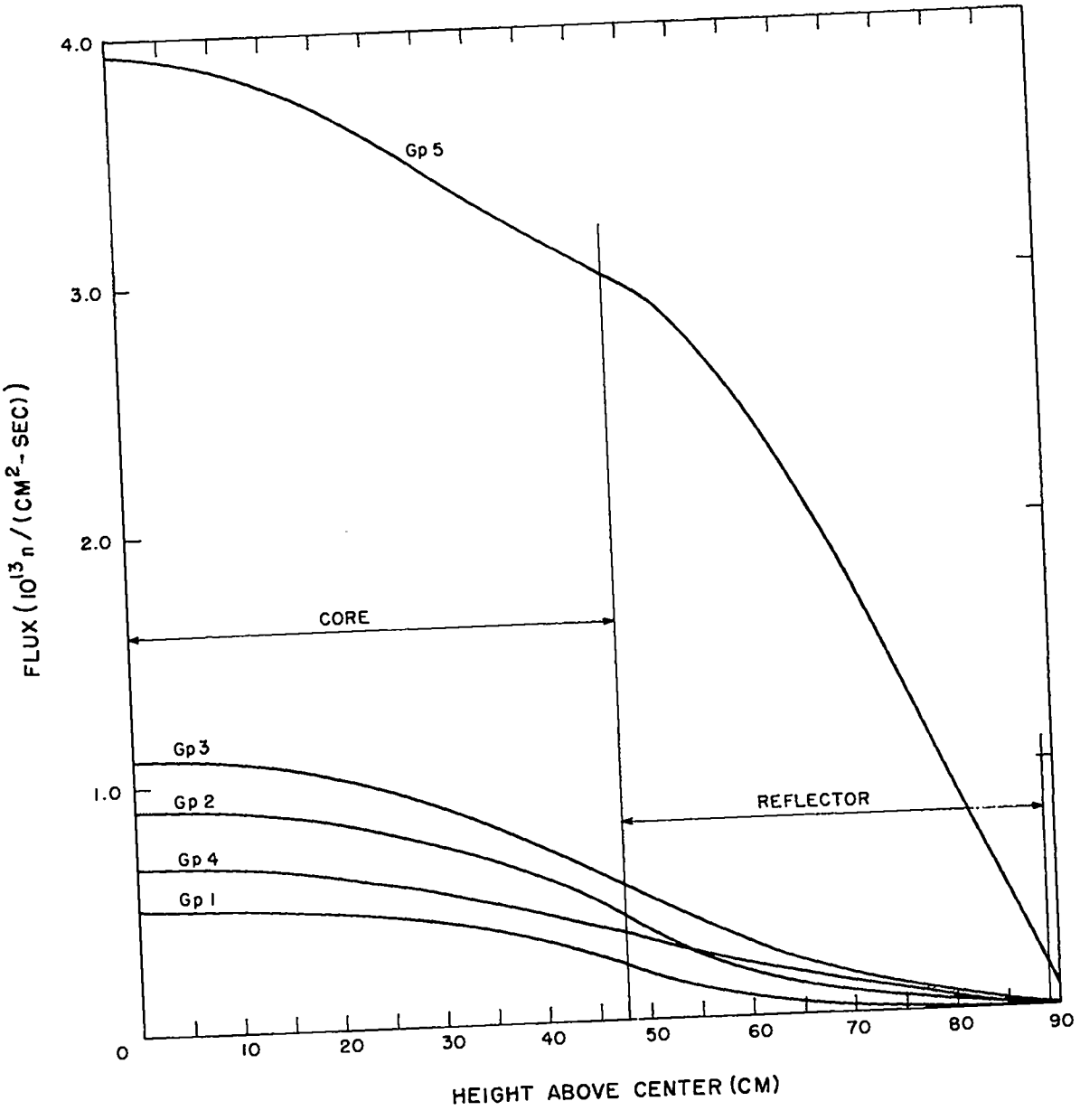

Fig. 5 Vertical fluxes, Region 3.

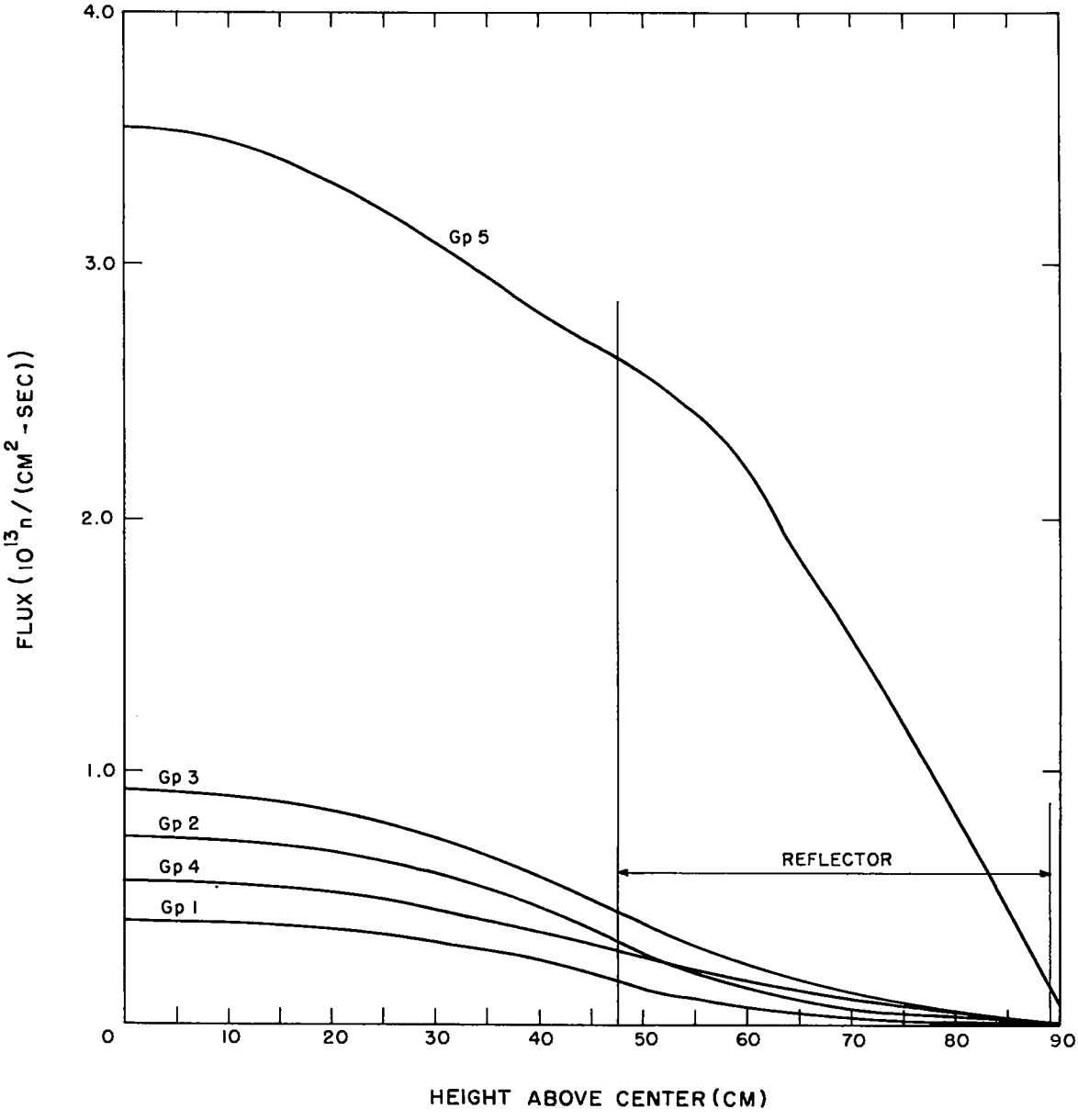

Fig. 6 Vertical fluxes, Region 4.

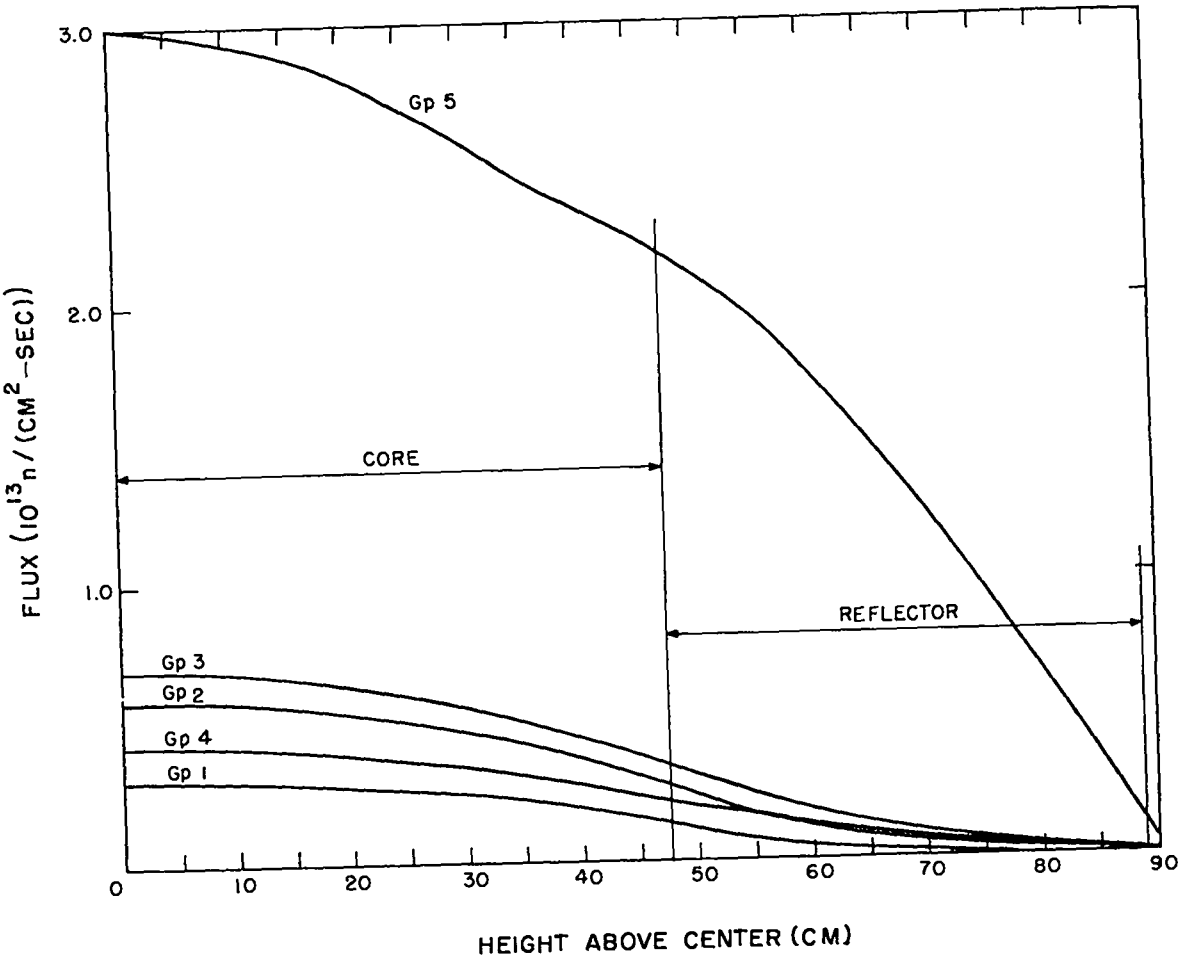

Fig. 7 Vertical fluxes, Region 5.

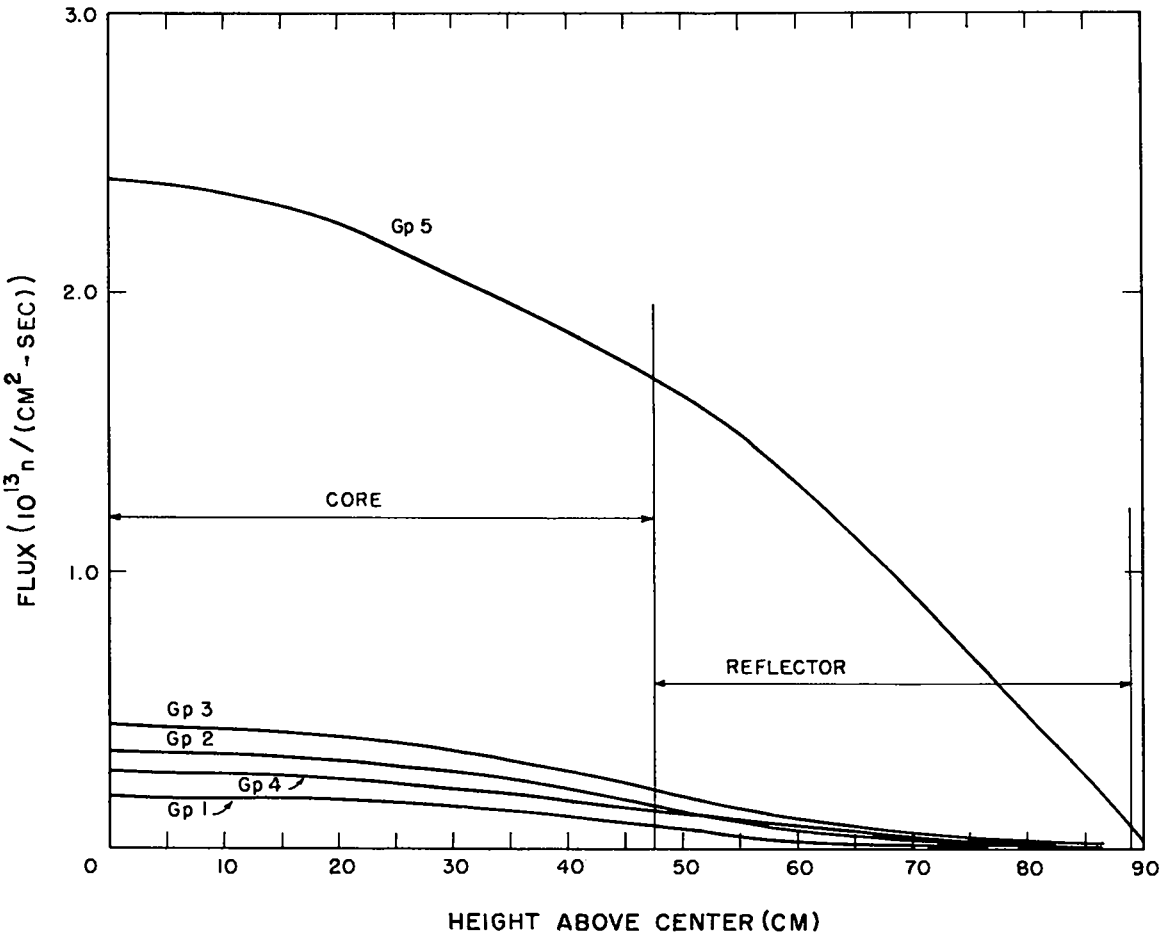

Fig. 8 Vertical fluxes, Region 6.

in the fuel element power illustrates the departure from linear burnup that occurs in the fuel channels. Since linear burnup was assumed in order to make the calculations, it would be expected that further calculations including adjusted fuel element burnups would lead to some corrections to the results. The variation in the total power per channel indicates that the fuel element flow rates would have to be varied from channel to channel in order to achieve the same total burnup of all the fuel elements.

III. Isothermal Temperature Coefficients

Isothermal temperature coefficients of reactivity were calculated for the 7.1 kg Turret loading previously selected as the standard 1350°C critical configuration. Contributions to the reactivity coefficients included the effects of cross section, dimensional, and material density changes, over a temperature range of 20°C to 1350°C. In addition the prompt reactivity effects associated with a change in fuel element temperature was investigated. Calculational procedures were the same as those used in making the critical mass estimates.

In the computations, it was assumed that the thermal absorption and fission cross-sections vary with temperature according to Eq. 9. Other effects of temperature upon cross-sections were neglected except for those changes brought about by the increase in the epithermal lower energy limit with temperature increase. This energy limit was taken to be the energy corresponding to the most probable velocity of the thermal neutrons at a given temperature. Room temperature (20°C) cross-sections are listed in Table IV for the epithermal and thermal groups (groups 4 and 5). These may be compared to the cross-sections at 1350°C listed in Table I. The effect of thermal expansion upon Turret dimensions and material densities was estimated using a linear expansion coefficient of 4.2×10^{-6} which is the specification for H4LM graphite over the range 20°C to 1350°C.[8]

Results from these first calculations are summarized in Table V.

Problem 43F is the reference criticality calculation at 1350°C. In problem 44 an intermediate cylinder calculation was performed in which 20°C cross-sections were used, but the vertical leakage cross-sections were the same as those used in 43F. In 44F the vertical leakage cross-sections were corrected to obtain room temperature values. The comparison of 44 and 44F illustrates the fact that the main contribution to the Turret temperature coefficient arises from the variation in thermal leakage with temperature change. The effect of thermal expansion is obtained from a comparison of problem 45 with problem 43F.

The temperature coefficients are listed in Table VI.

TABLE IV

FIVE GROUP CROSS-SECTIONS AT ROOM TEMPERATURE

Element	Group	σ_a	σ_{TR}	σ_f	$\sigma^{inel}_{g,g+1}$
Boron	4	1.878 + 02	6.075 + 01	0	6.498 - 02
	5	6.538 + 02	6.573 + 02	0	0
Carbon	4	8.380 - 04	4.340 + 00	0	7.906 - 02
	5	2.771 - 03	4.830 + 00	0	0
U^{235}	4	1.774 + 02	9.766 + 01	1.409 + 02	5.415 - 03
	5	5.809 + 02	5.909 + 02	4.890 + 02	0
U^{238}	4	2.907 + 01	1.518 + 01	0	7.581 - 03
	5	2.832 + 00	1.138 + 01	0	0

Cross-sections for groups 1, 2, and 3 are given in Table I.

TABLE V

TEMPERATURE EFFECT CALCULATIONS

Problem identification number	Temperature of cross-sections (°C)	Temperature of expansion (°C)	k_{eff}
43F	1350	20	1.0545
43G	1350	20*	1.0540
44	20	20	1.1930
44F	20	20	1.2542
45	1350	1350	1.0434

*Fuel elements expanded in length about 1.3%.

TABLE VI

TEMPERATURE COEFFICIENTS

Contribution	Temperature Range	% Δk	Reactivity Coefficient*
Cross-sections	20°C - 1350°C	20.0	1.30×10^{-4}
Expansion	20°C - 1350°C	1.1	0.08×10^{-4}
Total slow	20°C - 1350°C	21.1	1.38×10^{-4}
Prompt	20°C - ~3000°C	~0	~0

*Δk/k per °C

A comparison of 43G and 43F indicates that the thermal expansion contribution to the prompt temperature coefficient is negligible. In making the calculation, the effect of prompt expansion effects in the fuel was emphasized by allowing the fuel element rows to expand inward a total of 1 cm, which is the extension corresponding to about a 3000°C temperature rise in the fuel. (In the current Turret design a latch is placed at the outer end of each fuel channel; fuel elements abutt against this latch. Since the latch is attached to the bulk moderator, the fuel elements must expand inwards in the event of a prompt fuel temperature rise.)

A more exact estimate of the prompt fuel-temperature reactivity coefficient was subsequently carried out. A coefficient of -3×10^{-6} (Δk/k)/°C of fuel temperature rise was obtained. The moderator temperature coefficient, $[-1.4 \times 10^{-4}$ (Δk/k)/°C] is thus about 50 times as effective as the prompt reactivity effects produced by variation in fuel temperature. This factor of 50 is roughly equal to the ratio

$$\frac{\text{volume of graphite in moderator}}{\text{volume of graphite in fuel}}$$

The bulk moderator in Turret does make some contribution to the prompt reactivity coefficient, however, in that about 5% of the fission energy is deposited in the moderator by gamma rays and neutrons. One might estimate therefore that a total prompt coefficient might be as large as

$$\underset{\text{fuel}}{3 \times 10^{-6}} \text{ (Δk/k)/°C} + .05\underset{\text{moderator}}{[1.4 \times 10^{-4} \text{ (Δk/k)/°C}]} \cong 10^{-5} \text{ (Δk/k)/°C}$$

The overall $\Delta k = 21.1\%$ represents the amount of shutdown control that must be provided to overcome the temperature coefficient. It would be expected that an additional few percent in k of control would be required to overcome the effects of fission product poisoning and the power coefficient.

Other effects besides expansion may contribute to the prompt temperature coefficient. In particular, fission products, including xenon, samarium, and the delayed neutron precursors, may diffuse out of the fuel elements during a large temperature surge. No estimate has yet been made of the magnitude of reactivity changes which could be induced in this fashion.

IV. Control Rod Calculations

As previously noted, it is estimated that k_{eff} increases by 21.1% as the Turret reactor cools from its operating temperature of 1350°C to 20°C. Although the above estimate includes only effects due to isothermal temperature changes, it should represent the major contribution to the room temperature excess k which must be overcome by shutdown rods and/or other means. Because of the large amount shutdown Δk that must be provided, and because of the mechanical and materials problems associated with the introduction of rods into the high temperature rotating core of Turret, particular emphasis has been placed upon the control rod calculations for Turret. In addition, conservative allowances have been made for calculational uncertainties since there are no experimental data currently available on control rod measurements in reactors similar to Turret in general nuclear characteristics.

The rod calculations performed to date are described in two parts below. In Part 1, some initial calculations are described which were designed to investigate whether sufficient control could be achieved by using absorber rods in regions outside the core, i.e., in the central graphite plug and radial reflector. In Part 2, calculations which were performed on a system of three rings of rods are discussed. This configuration, which corresponds approximately to the control rod system that has been adopted for Turret, contains a ring of rods in each of the three principal radial regions: the central graphite plug, the core, and the radial reflector.

1. Survey Calculations. Four calculations were performed utilizing B. Carlson's new S_n code (DSN)[1]. The S_n option used was S_4. The results are shown in Table VII. Problem 50 was used as a reference problem for computing rod worths; thus, it contained no absorber rod materials. The specifications for this problem were the same as those for problem 44F (see Table V, Section III), except that a 4 in. o.d. central void region was used and a 1 in. annular void was interposed between the core and radial

TABLE VII

k_{eff} FOR VARIOUS CONTROL ELEMENT CONFIGURATIONS

Problem No.	Case	Rod Material	k_{eff}
50	No rods	---	1.22
51	4 in. o.d. central rod	B_4C	1.13
52	4 in. o.d. central rod plus 1 in. curtain between core and reflector	B_4C	0.85
53	4 in. o.d. central rod plus 1 in. curtain between core and reflector	Borated graphite	0.88

reflector. In problems 51 and 52, the rod material assumed was B_4C of density 2.5 g/cc; and, in problem 53, the material assumed was borated graphite containing 10 a/o boron enriched to 95% in B^{10}. The B^{10} atom densities for the two materials are 2.06×10^{22} per cc for B_4C, and 7.62×10^{21} per cc for the borated graphite. The rod materials considered for Turret use contain B^{10} densities comparable to the above densities.

Five-group radial flux plots obtained from calculations 50, 51, and 52 are illustrated in Figs. 9 and 10. Fluxes obtained from problem 53 were very similar to those shown in Fig. 10 from problem 52. It is seen in the figures that the absorption in the rods is strong enough to give effectively a complete suppression of the thermal and epithermal fluxes at the rod surfaces. The results indicate that sufficient control can be obtained using rods situated outside the core. It is expected, however, that some loss in effectiveness will be encountered in a more practical engineering design which must include clearances and some segregation of the material in the outer control curtain. As a hedge against these losses, the use of four or five smaller rods in the central plug rather than a large single rod would be recommended. More effectiveness should be achievable by placing the smaller rods as near to the inner surface of the core as is feasible. As is seen in the figures the thermal flux rises appreciably between the central rod and the core inner surface.

2. Worths of Control Rod Rings. Although the estimates of the worths in Turret of a 4 in. o.d. central rod, and a 1 in. thick control curtain, inserted between the core and radial reflector indicated sufficient control could be achieved by this arrangement, subsequent materials and design investigations led to the choice of a three-ring control-rod system composed of

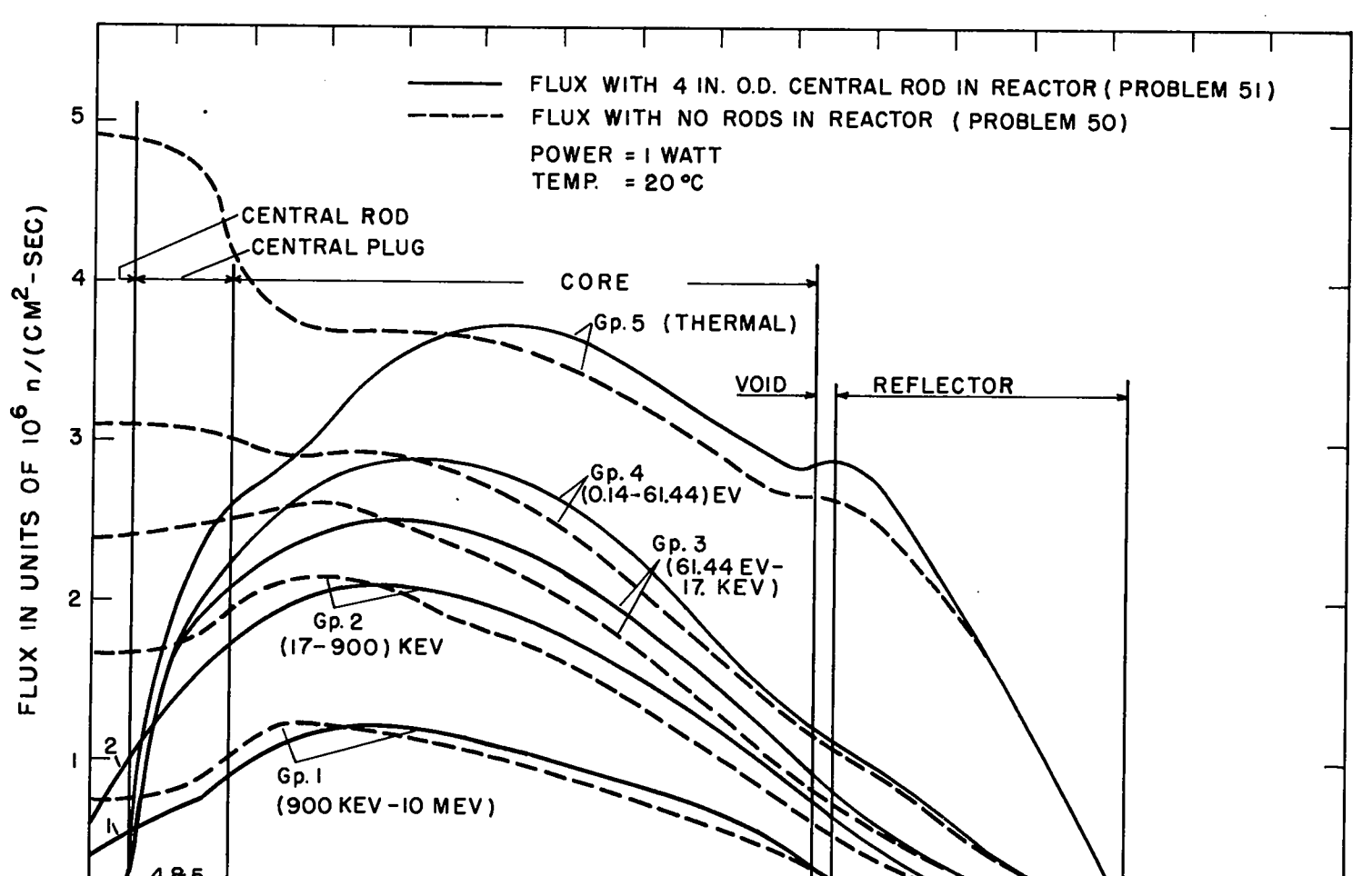

Fig. 9 Central rod flux perturbations.

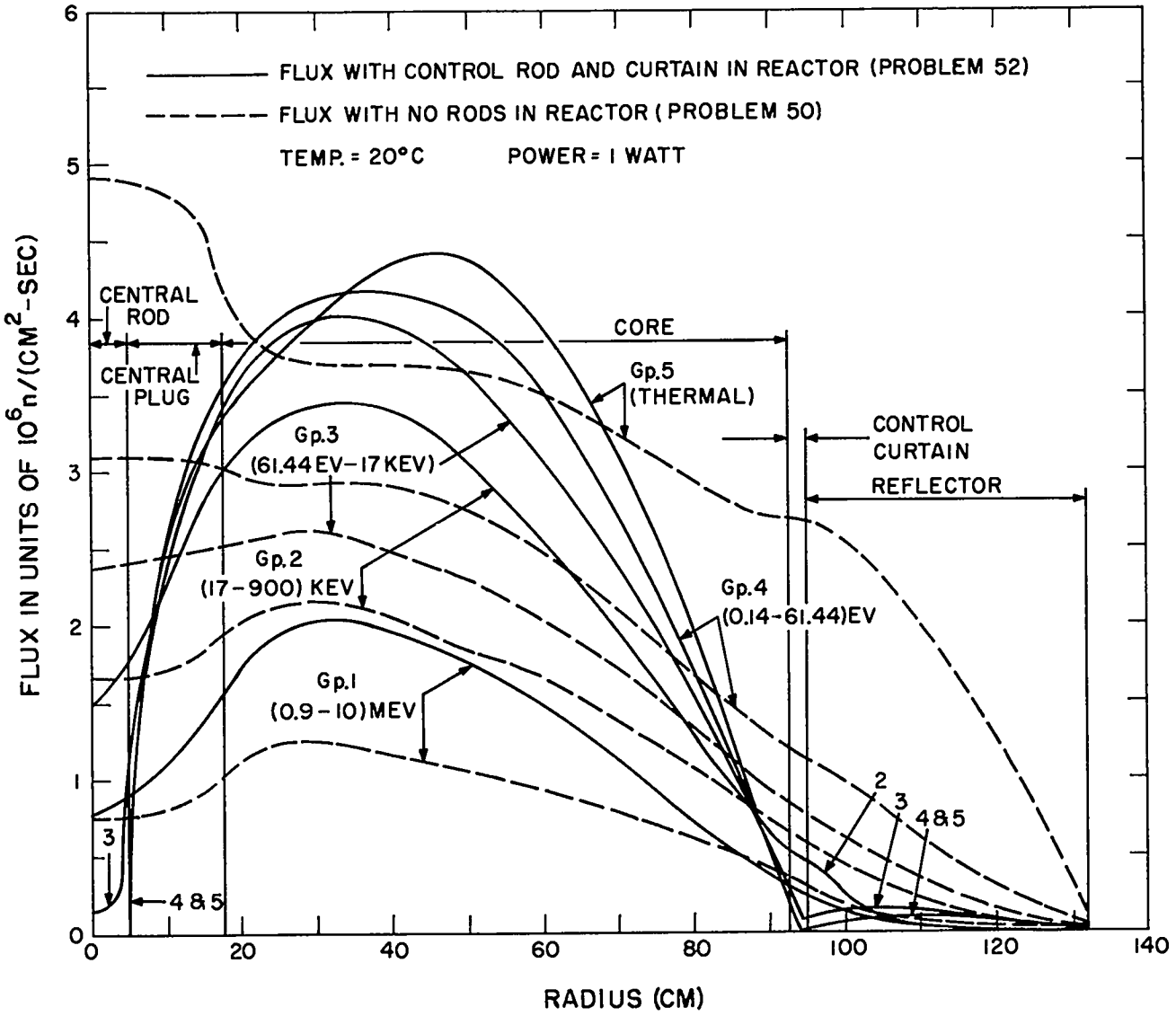

Fig. 10 Central rod and control curtain flux perturbations.

1-1/4 in. o.d. ZrB_2 cylindrical rods. In this system, a ring of five rods is situated on a 3.5 in. radius in the stationary central plug, a second ring of six rods is inserted on a 20.5 in. radius in the rotating core, and a third ring of five rods is located in the stationary radial reflector on a radius 3-in. outside the core periphery. The calculations reported herein indicate that the sixteen-rod, three-ring system should provide sufficient shutdown control for Turret with reasonable allowances made for calculational error and for the malfunction of one or two rods in the system.

Reduction to Two-group, One-region Model. Two-group diffusion theory calculations have been used extensively for estimating the worths of rings of cylindrical rods in thermal reactors.[6,9] Usually the two-group theory is applied to a one-region, or at most, two-region system since the analytic solutions become very unwieldly if more groups or regions are considered. For these reasons, and since the geometry of a ring of control rods is not easily adaptable to the numerical type of machine calculation, a two-group, one-region model has been used for estimating rod worths in Turret.

To homogenize the Turret core and central plug regions, five-group FIRE code calculations were performed on a homogeneous core and reflector model in which the fuel concentration in the core was determined by requiring that the simplified two-region model give the same k_{eff} as the more detailed calculational model described in Section II.3. Specifically, the room temperature case, problem 44F in Section III, was taken as the reference problem. The original average fuel concentration, 0.00279 g/cc Oy, turned out to be the correct one to use in the simplified model.

Secondly, the five-group constants were collapsed to obtain constants for the two-group equations

$$\begin{aligned} D_1\nabla^2\varphi_1 - \Sigma_{a1}\varphi_1 - \Sigma_{1,2}\varphi_1 + \nu\Sigma_{f1}\varphi_1 + \nu\Sigma_{f2}\varphi_2 &= 0 \\ D_2\nabla^2\varphi_1 - \Sigma_{a2}\varphi_2 + \Sigma_{1,2}\varphi_1 &= 0 \end{aligned} \qquad (12)$$

using the collapsing procedure described in Section II.2. In Eq. 12 the D_i, Σ_{ai}, Σ_{fi}, and φ_i, i = 1, 2, are diffusion coefficients, absorption and fission cross-sections, and fluxes, respectively, with i = 1 referring to the fast group and i = 2 referring to the thermal group. The group transfer cross-section, $\Sigma_{1,2}$, was adjusted in value so that the buckling μ^2 of the two-group buckling solutions μ^2 and η^2 to Eq. 12

$$\mu^2, \eta^2 = \frac{1}{2}\left\{\left[(\alpha - \beta)^2 + 4s\right]^{1/2} \mp (\alpha + \beta)\right\}$$
$$\alpha = \Sigma_{a2}/D_2, \beta = \left(\Sigma_{a1} + \Sigma_{12} - \nu\Sigma_{f1}\right)/D_1, S = \nu\Sigma_{f2}\Sigma_{12}/D_1D_2 \qquad (13)$$

gave a correct $J_0(\mu r)$ fit to the five-group thermal flux in the core. In Eq. 13 ν is treated as an eigenvalue where

$$\nu = \nu'/k_{eff} \qquad (14)$$

in which ν' is the number of neutrons released per fission.

The two-group constants generated by the above procedure are tabulated below:

TABLE VIII

TURRET TWO-GROUP CONSTANTS

	Core		Reflector	
	Fast	Thermal	Fast	Thermal
D	1.324	0.8730	1.179	0.8599
Σ_a	1.320×10^{-3}	4.204×10^{-3}	4.154×10^{-4}	5.844×10^{-4}
Σ_f	3.667×10^{-4}	3.389×10^{-3}	0	0
Σ_{12}	2.155×10^{-3}		2.155×10^{-3}	

$\nu' = 2.46$ $\quad k_{eff} = 1.2342$

These constants were used to calculate the radial flux plots shown in Fig. 11. The calculational procedure used is that described by Murray.[10] Vertical leakage allowances are included in the core Σ_a's of Table VIII which include group leakage cross-sections collapsed from the five-group case. It is seen in Fig. 11 that adequate agreement is obtained between the five-group and two-group fluxes.

Two-group Control-ring Code. A FORTRAN code, ROD1, was set-up for obtaining solutions to the control ring problem on the 704 computer. The critical determinant for the case of a ring of M rods in a bare core is reproduced in Appendix I from reference 11. The ROD1 code solves the

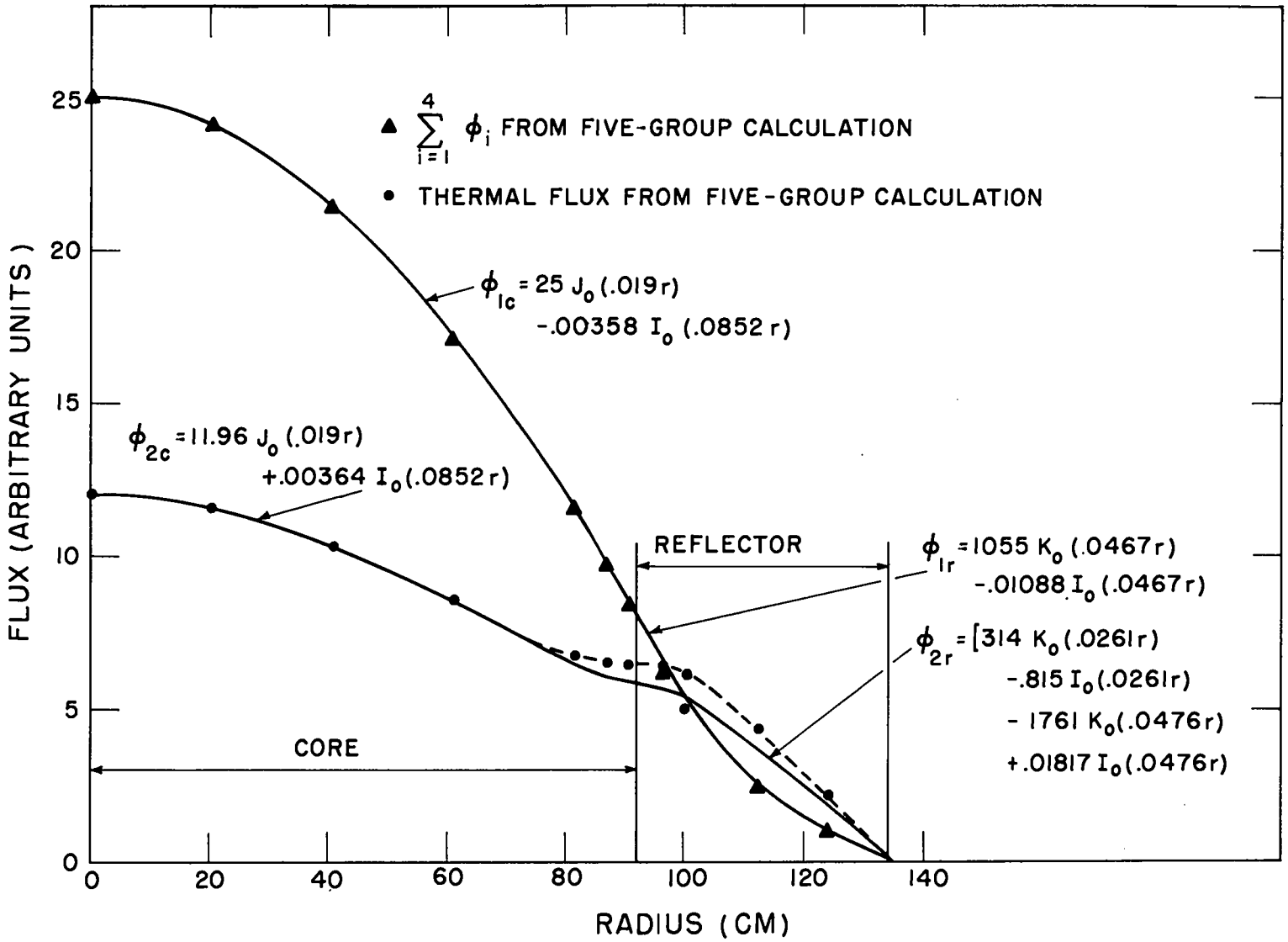

Fig. 11 Comparison of five-group and two-group fluxes.

critical determinant from a given set of input data including:

(a) the core constants listed in Table VIII,
(b) the core extrapolated radius, R,
(c) the rod radius, a,
(d) the number of rods in the ring, M,
(e) the ring radius, d,
(f) two initial guesses for k_{eff},
(g) convergence criteria,
(h) the order of approximation, L, and
(i) the fast and thermal rod extrapolation distances d_1 and d_2, respectively.

For the case of no control rods in the bare equivalent core, the radial buckling is determined by

$$\mu^2 = (2.405)^2/R^2, \tag{15}$$

where R is the extrapolated core radius, and k_{eff} is then fixed by Eq. 13 and 14. With rods inserted in the core, ROD1 iterates on k_{eff} by linear extrapolation until the critical determinant vanishes within the desired convergence criteria. Comparison of the cases with and without rods establishes the rod worths.

The ROD1 code is generally applicable to the ring problem except that for rings containing 16 or more rods the high order Bessel functions obtained have values exceeding the capacity of the 704 computer. The case of a single central rod is solved by setting L = 0, M = 1, and the ring radius equal to zero. Experience has shown that convergence will not be achieved if the initial guesses for k_{eff} are too low compared to the correct value. Generally, for a noncentral rod or ring of rods, the second order approximation, L = 1, produces sufficient accuracy, but the code will compute orders up to L = 9 if the Bessel function limitation cited above is not exceeded.

Rod Extrapolation Distances. Five-group DSN (S_4) calculations were used for estimating the rod extrapolation distances, d_1 and d_2. The geometry in the computations was that of a central rod in the bare equivalent core. In the eight cases considered, the rod parameters were varied as described in the following table:

TABLE IX

CENTRAL ROD WORTHS

Problem Number	Rod o.d. (in.)	Rod Material	Rod Worth (% Δk)	d_1 (cm)	d_2 (cm)
71F	7/8	ZrB_2 (0.621 g/cc) natural boron	2.66	11.04	3.175
71D	1	ZrB_2 (0.621 g/cc) natural boron	3.03	9.959	3.293
71K	7/8	ZrB_2 (4.65 g/cc) natural boron	3.14	7.085	3.225
71I	1	ZrB_2 (4.65 g/cc) natural boron	3.37	7.233	3.432
71M	1-1/8	ZrB_2 (4.65 g/cc) natural boron	3.55	7.376	3.760
71L	1-1/4	ZrB_2 (4.65 g/cc) natural boron	3.66	8.138	4.108
71E	1	B_4C (2.5 g/cc) natural boron	3.64	5.979	3.403
71J	1	ZrB_2 (4.65 g/cc) boron enriched to 85% in B^{10}	3.87	8.138	4.108

A second FORTRAN code, ROD2, was devised for computing d_1 and d_2 from the DSN results. ROD2 contains a subroutine which is a two-group version of the FIRE code modified to solve the central rod case. Flux calculations start at the rod boundary, $r = r_0$, from the boundary condition

$$d = \varphi\left(r_0\right)/\varphi'\left(r_0\right) \tag{16}$$

where d is the appropriate group rod extrapolation distance. In terms of the FIRE code flux solution

$$\varphi_n = \alpha_n \varphi_{n+1} + \beta_n \tag{17}$$

for the nth space point (Eq. 18 of LA-2161, p. 18), the starting conditions at the rod boundary are

$$\alpha_0 = \frac{2}{2\left(1 + \frac{\Delta r}{d}\right) - \frac{C\Delta r^2}{r_0 d} + \frac{a\Delta r^2}{D}}$$

$$\beta_0 = b\,\alpha_0\,\Delta r^2/2D \qquad (18)$$

The definitions of the terms in the above equations and the remaining procedures for the diffusion problem, as incorporated in ROD2, are described in LA-2161.[2]

Using the diffusion theory solutions, ROD2 further iterates on d_1 and d_2 (by linear extrapolation from initial guesses) until the relative changes in the group neutron losses, due to inserting the rod, satisfy

$$\frac{L_1' - L_1}{L_1 + L_2} = \sum_{g=1}^{4}\left(l_g' - l_g\right)\Big/\sum_{g=1}^{5} l_g$$

$$\frac{L_2' - L_2}{L_1 + L_2} = \left(l_5' - l_5\right)\Big/\sum_{g=1}^{5} l_g \qquad (19)$$

where L_1 and L_2 are the normalized two-group neutron losses (due to absorption and escape) and l_g, $g=1,\ldots,5$ are the normalized five group losses obtained in the DSN calculations. The primed losses refer to the case with the rod inserted in the bare core, and unprimed losses are for the case of no rods in the core. Thus the two group neutron balance conditions above give criteria for computing d_1 and d_2 and at the same time meet the condition that the correct Δk be obtained since

$$\Delta K/K = 1 - 1/(1 + \Delta L/L) \cong \Delta L/L \qquad (20)$$

where L now represents the total losses.

The fluxes in the control rod as obtained from the S_4 calculations for cases 71D, E, I, and J are illustrated in Fig. 12. The flux discontinuities at the rod boundary, particularly in the case of the thermal flux, illustrate the desirability of using a transport theory approach to obtain rod extrapolation.

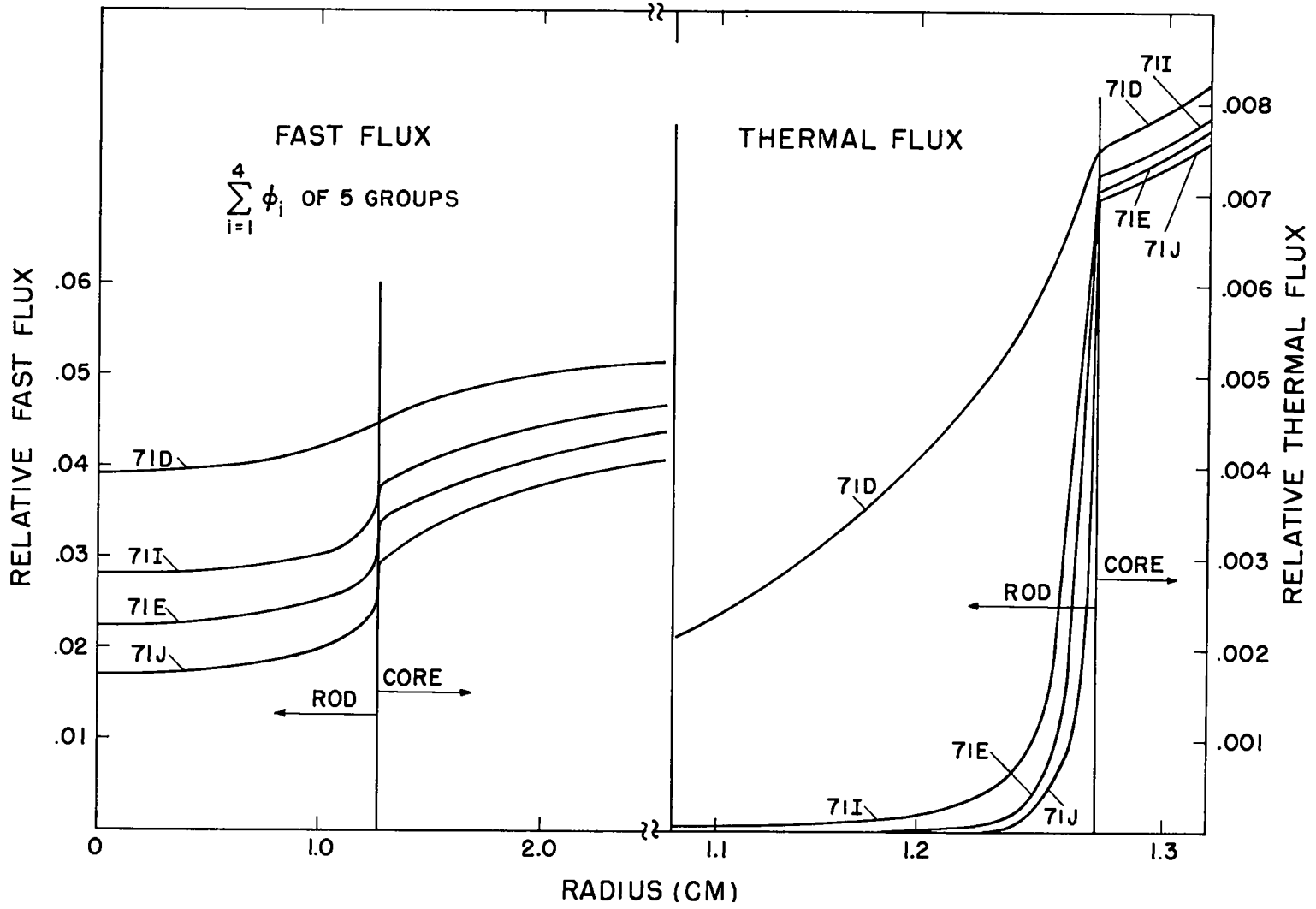

Fig. 12 Control rod fluxes.

distances. Figures 13a and 13b show the effect of varying the B^{10} concentration and the rod radius on the extrapolation distances. It is seen that practically all of the change in rod worth for the given range of absorber density is due to the change in the epithermal absorbtion in the rod (represented by change in d_1). Consequently, the massive boron densities represent an uneconomic use of poison, but it is highly desirable from the mechanical standpoint to minimize the number of rods in Turret.

Ring Worths. Worths of the three rings described in Table X below are tabulated in Table XI as computed by ROD1 using the extrapolation distances for the eight rod cases described in Table IX.

TABLE X

RING PARAMETERS

Description	Number of Rods, M	Ring Radius, d
Plug ring	5	8.89 cm
Core ring	6	52.07 cm
Reflector ring	5	98.11 cm

TABLE XI

RING WORTHS (% Δk)

Rod Case	Ring Worths			Total Worth
	Plug Ring	Core Ring	Reflector Ring	
71F	8.38	9.76	3.64	21.78
71D	9.13	11.18	4.14	24.45
71K	9.31	11.56	4.30	25.17
71I	9.74	12.47	4.63	26.84
71M	10.00	13.12	4.86	27.98
71L	10.17	13.47	4.98	28.62
71E	10.19	13.47	4.99	28.65
71J	10.56	14.35	5.32	30.23

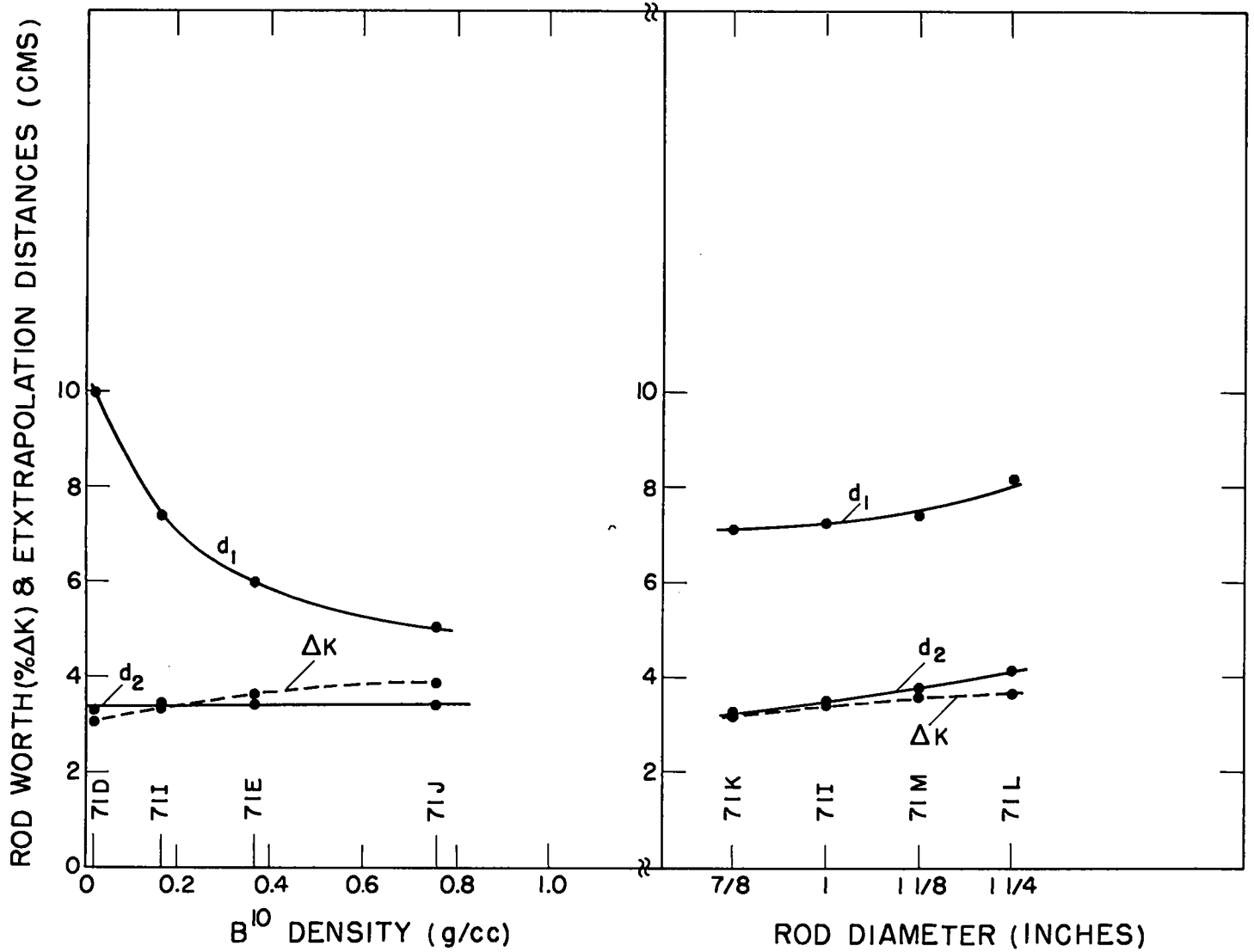

Fig. 13a Central rod worth and extrapolation distances vs B^{10} concentration.

Fig. 13b Central rod worth and extrapolation distances vs rod diameter.

The reflector rod worths as computed by ROD1 were corrected by the factor

$$f = \varphi_R^2(d)/\varphi_B^2(d) = 2.97$$

where $\varphi_R(d)$ is the unperturbed thermal flux at the ring radius in the reflected case, and $\varphi_B(d)$ is the same flux in the bare equivalent core.

The 1-1/4 in. rod, case 71L, has been tentatively adopted for use in Turret since it does not require the use of enriched boron to give sufficient shutdown control. Since it is estimated that approximately 21% Δk of control will be needed to shutdown Turret from full operation at 3 MW and 1350°C to room temperature, a 7% Δk safety factor will be available as an allowance for calculational error, or for the malfunction of some rods. Additional control may be readily achieved by increasing the number of rods in the reflector ring if future investigations indicate more control is needed.

The worths of the rings are plotted in Fig. 14 in terms of the number of rods in the ring for case 71L. It is seen that in the central plug, negative rod shadowing (ring worth less than M times values of one rod) occurs due to the close spacing of the rods. In the core and reflector rings, on the other hand, positive shadowing occurs.

V. Miscellaneous Reactor Kinetics Considerations

Some rough estimates have been made which indicate qualitatively the behavior of Turret following a loss of coolant flow during operations at 3 MW. It was assumed that the prompt temperature coefficient of reactivity associated with the fuel is ~ zero, so that power generation continues, without any sudden decrease, at the 3 MW level. The heat capacity of the fuel elements should limit the initial fuel element temperature rate of rise to 10°C/sec. Since the neutron temperature is determined primarily by the bulk moderator temperature and since the moderator heat capacity is 40-50 times greater than the capacity of the fuel elements, it is expected that the fuel element temperatures would rise to a high level before the slowly-acting reactivity coefficient associated with moderator temperature would shut off the power. However, it appears at least 10-20 seconds of time is available for inserting control rods before the fuel element temperatures become uncomfortably high.

In connection with the above, the possibility of diffusion of fission product poisons out of the fuel elements during a fuel element temperature rise should be considered. In this event a power surge would be initiated if the poisons escaped the core. It is expected that the power rise would depend upon the amount of reactivity insertion and upon the shut off mechanism

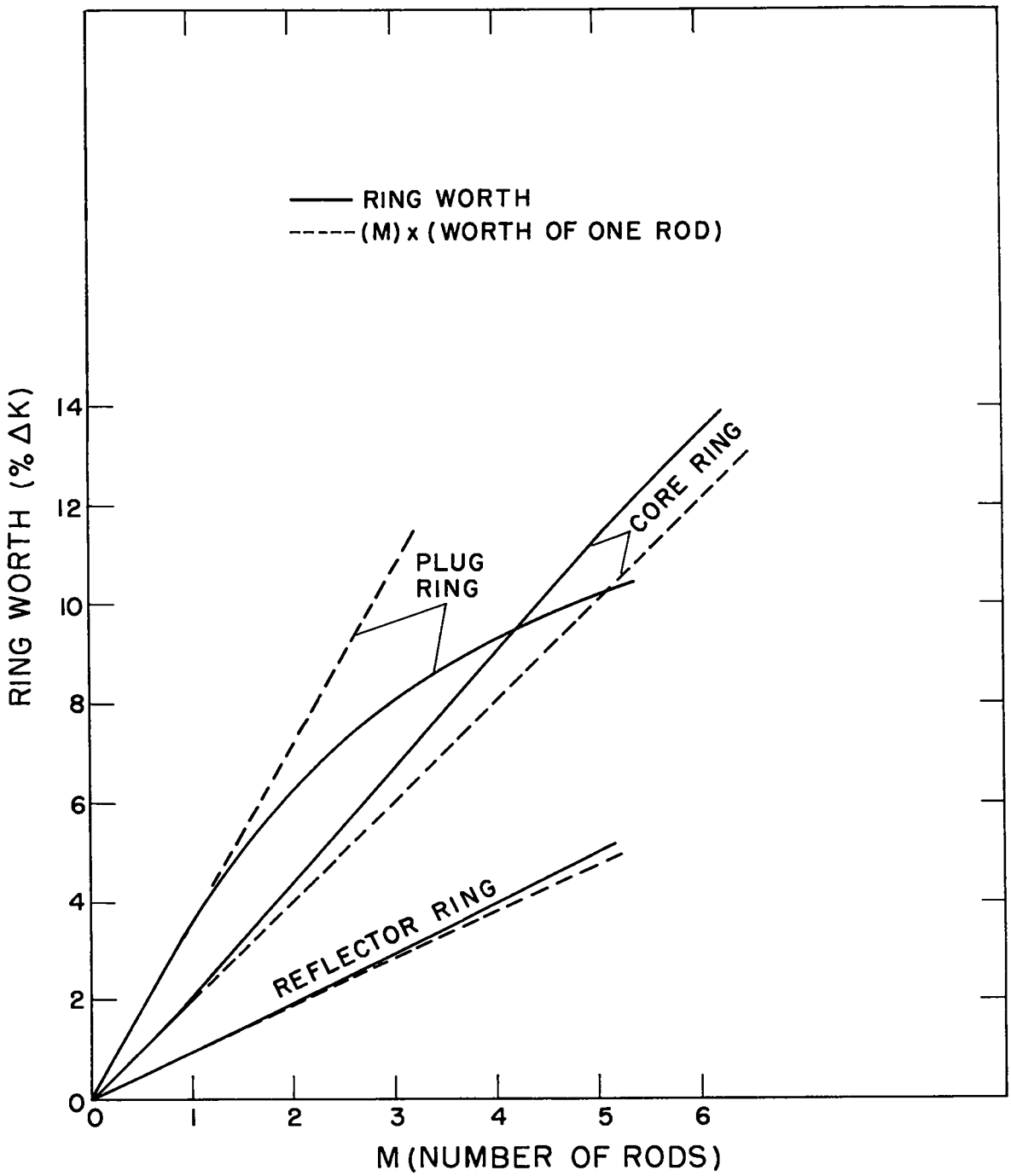

Fig. 14 Ring worths vs number of rods, M, in rings [Case 71L: 1 1/4" dia ZrB_2 rods (4.65 g/cc - natural boron)].

associated primarily with the 5% of fission energy which is deposited promptly in the bulk moderator via elastic scattering of the prompt neutrons and attenuation of the prompt fission gammas.

Some calculations have been made in an attempt to predict the fission product inventory as a function of operating time, and hence the poison level, in Turret, but these estimates are of limited reliability because diffusion rates of fission products as a function of temperature are not known. The wide range of temperatures existing in the Turret core is a further complication, since important poisons may be effectively held up in the cooler portions during normal operations, while in the hotter portions the concentration of these same poisons may be much lower.

APPENDIX I

THE CRITICAL DETERMINANT FOR A RING OF CONTROL RODS IN A BARE CORE

The application of the condition that the fluxes vanish at the extrapolated radius of the bare core, and the rod boundary conditions (Eq. 16), to the two-group diffusion equations (Eq. 12) yields the critical determinant for a ring of rods. The detailed method of analysis is given in reference 12, and the critical determinant in the form described below is reproduced from reference 11. To the Lth approximation the determinant is

$$\sum_{n=0}^{L} \left(A_{kn}\delta_{kn} - B_k T_{kn}\right) = 0 \qquad k = 0, 1, 2, \ldots, L$$

where

$$A_{kk} = a_{32k}a_{44k} - a_{34k}a_{42k}$$

$$B_k = a_{31k}a_{44k} - a_{34k}a_{41k}$$

$$\delta_{kn} = 1, \quad n=k$$

$$= 0, \text{ otherwise}$$

$$a_{31k} = (-1)^k \left[\left(1/d_1 - k/a\right) J_k(\mu a) + J_{k+1}(\mu a)\right]$$

$$a_{32k} = \left(1/d_1 - k/a\right) Y_k(\mu a) + Y_{k+1}(\mu a)$$

$$a_{34k} = \left(1/d_1 - k/a\right) K_k(\eta a) + K_{k+1}(\eta a)$$

$$a_{41k} = (-1)^k S_1 \left[\left(1/d_2 - k/a\right) J_k(\mu a) + J_{k+1}(\mu a)\right]$$

$$a_{42k} = S_1 \left[\left(1/d_2 - k/a \right) Y_k(\mu a) + Y_{k+1}(\mu a) \right]$$

$$a_{44k} = S_2 \left[\left(1/d_2 - k/a \right) K_k(\eta a) + K_{k+1}(\eta a) \right]$$

with the coupling coefficients defined as

$$S_1 = \Sigma_{1,2} / \left(\Sigma_{a2} + D_2 \mu^2 \right)$$

$$S_2 = \Sigma_{1,2} / \left(\Sigma_{a2} - D_2 \eta^2 \right)$$

and

$$T_{kn} = \sum_{s=0}^{\infty} \left[M \cdot J_{Ms+k}(\mu d)\ J_{Ms-n}(\mu d)\ Y_{Ms}(\mu R) / J_{Ms}(\mu R) \right] - L_{kn}$$

$$L_{kn} = \sum_{m=2}^{M} Y_{k+n}\left(\mu r_{1m} \right) \cos\ p_{kn}$$

$$\cos\ p_{kn} = \cos\ \pi\ (n - k) \left(\frac{m - 1}{M} + \frac{1}{2} \right)$$

in which the bucklings μ^2 and η^2 are defined by Eq. 13, r_{1m} is the linear distance from a reference rod to the mth rod in the ring, and the other constants are defined in the text. In the expansion of T_{kn}, ROD1 applies a term ratio test for selecting the number of terms required to meet a convergence criteria which is specified on input.

APPENDIX II

EXCERPTS FROM LASL INTERNAL MEMORANDA

Pertinent data from LASL internal reports are reproduced herein for the benefit of readers who do not have access to these reports:

3. Byers, C. C., "Graphite-Moderated, Graphite-Reflected Critical Assemblies," N-2-529.

> .....The first system built up on the assembly machine utilized the maximum volume possible and consisted of a 4 ft. cubic core surrounded by a 1 ft. thick graphite reflector. In this configuration, the critical mass is 7.985 kg of oralloy (uranium enriched to 93.2 w/o U^{235}) distributed in the form of 0.001 in. by 2.8 in. by 7.5 in. foils throughout the moderating graphite to give a C/Oy atomic ratio of 6650. The effective density of the graphite in the reflector is 1.55 gm/cm^3 while that of the core is 1.50 gm/cm^3. The building up of the fuel subassemblies from a number of graphite plates results in a lower average density than for the single pieces used in the reflector.....
>
> .....The effect of self shielding in the oralloy foils may be determined by replacing a number of the 0.001 in. foils by an equivalent weight of 0.002 in. foils and measuring the effect of such an interchange on the reactivity of the system. This was done for a number of foils and the effect from a 100% interchange was estimated to be approximately -890 cents.....

7. MacMillan, D. P., "Interim Data on H4LM Graphite," N-1-158.

> .....No detailed analyses of molded H4LM are available, but since extruded and molded H4LM use the same raw materials, an ash analysis of extruded H4LM is given below:

S	.05%
Fe_2O_3	.2
NiO	.002
CaO	.04
Al_2O_3	.01
TiO_2	.01
V (Believed to be less than 100 ppm and guessed to be 70 or 80 ppm)	
SiO_2	.1
B	Approximately 1 ppm
Total	.41+

REFERENCES

1. Carlson, B., Lee, C., and Worlton, J., "The DSN and TDC Neutron Transport Codes," LAMS-2346, February 12, 1960.

2. Mills, C. B., and Brinkley, F., "A One-Dimensional Intermediate Reactor Computing Program," LA-2161, March 27, 1959.

3. Byers, C. C., "Graphite-Moderated, Graphite-Reflected Critical Assemblies," Internal Report, N-2-529.*

4. Mills, C. B., "Physics of Intermediate Reactors," LAMS-2288, March 31, 1959.

5. Foderaro, A., "An Iteration Method for the Specification of Multigroup Bucklings," Nuclear Science and Engineering 6, 6 (1959).

6. "Reactor Physics Constants," ANL-5800, July 1, 1958.

7. MacMillan, D. P., "Interim Data on H4LM Graphite," Internal Report, N-1-158.**

8. Eatherly, W. P. et al., "Physical Properties of Graphite Materials for Special Nuclear Applications," Paper P/708, Second International Conference on the Peaceful Uses of Atomic Energy, Geneva, 1958.

9. "Reactor Control Meeting Held in Los Angeles, March 6-8, 1957." TID-7532, Part 1, October 1957.

10. Murray, R. L., Nuclear Reactor Physics, Prentice Hall, Inc., Englewood Cliffs, N. J., 1957, p. 110.

11. Murray, R. L., "Reactivity Values of Multiple Reactor Control Rods," Paper presented at the Nuclear Engineering and Science Congress, sponsored by Engineers Joint Council, December 12-16, 1955, at Cleveland, Ohio. Preprint 83, published by American Institute of Chemical Engineers, New York, N. Y.

12. Garabedian, H. L., "Control Rod Theory for a Cylindrical Reactor," AECD-3666, Westinghouse Atomic Power Division, Pittsburgh, Pa., August 9, 1950.

---

*Pertinent information from this internal report can be found in Appendix II.

**Pertinent information from this internal report can be found in Appendix II.